

Analytical Charge Voltage Model in MOS Inversion Layer Based on Space Charge Capacitance

MA Yu-tao(马玉涛), LIU Li-tian(刘理天) and LI Zhi-jian(李志坚)

(*Institute of Microelectronics, Tsinghua University, Beijing 100084, China*)

Abstract: The concept of Space Charge Capacitance (SCC) is proposed and used to make a novel analytical charge model of quantized inversion layer in MOS structures. Based on SCC, continuous expressions of surface potential and inversion layer carrier density are derived. Quantum mechanical effects on both inversion layer carrier density and surface potential are extensively included. The accuracy of the model is verified by the numerical solution to Schrodinger and Poisson equation and the model is demonstrated, too.

Key words: MOS structure; charge voltage model; space charge capacitance; quantum mechanical effects; analytical model

EEACC: 2530F; 2560B

CLC number: TN386 **Document code:** A **Article ID:** 0253-4177(2000)10-0955-07

1 Introduction

The 2-Dimensional nature of the inversion layer carrier in MOS structure is well-known^[1,2] and the Quantum Mechanical Effects (QMEs) on MOS structure's behavior have been extensively studied by numerical survey by self-consistent solution to Schrodinger and Poisson equations^[3], experimental investigation^[4] and analytical modeling study^[5]. Among all the studies, analytical models are used to clarify the physical principles underlying QMEs on MOS devices characteristics. In Reference [6], the authors attempted to model the intrinsic capacitance of an inversion layer considering the finite charge layer thickness based on the numerical calculation results and have presented an explicit charge-voltage expression in MOS inversion layer. However, the threshold voltage shift effect due to the QMEs^[5] was not considered in their model, nor was the surface potential which has experienced a significant change in respect to the semiclassical description^[7]. In Reference [8], QMEs are involved in the compact model based on the experimental results of Reference [9]. However, the calculation of surface potential and charge

MA Yu-tao (马玉涛), Ph. D. candidate. His work focuses on physics of deep sub-micron devices, modeling, simulation and relevant technology research.

LIU Li-tian(刘理天), Professor. His present research focuses on the development of integrated sensors and MEMS.

Received 28 January 2000, revised manuscript received 1 May 2000

density needs iteration so that the application of the model is limited. In Reference [10], an analytical charge model is presented based on the model in Reference [9]. However, the whole model was developed in a semiclassical frame but not like a physical model because of the effects of threshold voltage shift, inversion layer thickness and the increase in depletion charge density due to the increased surface potential.

In this paper, a newly developed, closed-form comprehensive charge-voltage model of MOS inversion layer is presented. A new concept of Space Charge Capacitance (SCC) is proposed as the base of the model. Explicit expressions are derived considering the surface potential, the inversion layer's charge sheet density from depletion to weak and the strong inversion with smooth transition characteristics. QMEs are involved in the model in three aspects: threshold voltage shift due to QMEs, following our recent work^[5], the finite inversion layer thickness, and the increase in depletion layer charge after the strong inversion point due to increased surface potential. The latter two aspects are modeled on the basis of numerical results of self-consistent solution to Schrodinger and Poisson equations^[3].

2 Model Description

The base of the development of new model is the concept of Space Charge Capacitance (SCC), which is defined as:

$$C_{\text{charge}} = (Q_{\text{inv}} + Q_{\text{d}}) / (Q_{\text{inv}}/C_{\text{inv}} + Q_{\text{d}}/C_{\text{d}}) \quad (1)$$

where Q_{inv} and Q_{dep} are carrier sheet density and depletion charge sheet density, respectively. C_{inv} and C_{dep} are inversion layer capacitance and depletion layer capacitance, respectively. The physical meaning is the overall capacitance of the space charge region in semiconductor. It consists of two parts: the inversion layer capacitance C_{inv} and depletion layer capacitance C_{dep} . But the two capacitors are neither parallel nor serial connected since both the total charge and total potential are the sum of the two components.

Thus, the total gate charge of MOS structure can be given as:

$$C_{\text{gate}} = C_{\text{ox}} C_{\text{charge}} / (C_{\text{ox}} + C_{\text{charge}}) \quad (2)$$

The surface potential is:

$$\Phi_{\text{s}} = C_{\text{ox}} V_{\text{gate}} / (C_{\text{ox}} + C_{\text{charge}}) \quad (3)$$

The inversion layer charge density is:

$$Q_{\text{inv}} = C_{\text{ox}} C_{\text{charge}} V_{\text{gate}} / (C_{\text{ox}} + C_{\text{charge}}) - Q_{\text{dep}} \quad (4)$$

In order to get rid of the coupling of Eq. 1 and Eq. 4, Q_{inv} in Eq. 1 is approximated by: $Q_{\text{inv}} = C_{\text{oxeff}} V_{\text{gsteff}}$ with $C_{\text{oxeff}} = C_{\text{ox}} C_{\text{inv}} / (C_{\text{ox}} + C_{\text{inv}})$. V_{gsteff} is given in Ref. [11].

The next step is to accurately model the inversion charge capacitance C_{inv} . The inversion charge capacitance is given by:

$$C_{\text{inv}} = \epsilon_0 \epsilon_{\text{Si}} / X_{\text{dc}} \quad (5)$$

where X_{dc} is the inversion layer thickness.

According to the numerical results by solving Schrodinger and Poisson equations self-consistently, the inversion layer thickness is modeled as:

$$X_{\text{dc}} = (b_1 + b_2 E_{\text{eff}}) / (b_3 + E_{\text{eff}}) \quad (6)$$

where the unit of E_{eff} is MV/cm. $b_1(5.047)$, $b_2(0.771)$ and $b_3(0.113)$ are determined by fitting the numerical results. E_{eff} in Eq. 6 is the effective electric field given as below:

$$E_{\text{eff}} = (V_{\text{gtx}} + \alpha(V_{\text{th}} - V_{\text{FB}} - \phi_0)) / (2T_{\text{ox}}) \quad (7)$$

where V_{th} is the threshold voltage, V_{FB} is the flatband voltage and ϕ_0 is the surface potential at the threshold point. T_{ox} is the gate oxide thickness. The coefficient α in Eq. 9 is chosen as 8. V_{gtx} is given by Ref. [6]:

$$V_{\text{gtx}} = \eta \phi \ln(1 + \exp((V_{\text{gate}} - V_{\text{th}}) / \eta \phi)) \quad (8)$$

where η is the subthreshold swing parameter, ϕ is the thermal voltage.

The numerical and model results of X_{dc} are shown in Fig. 1 with respect to E_{eff} . The universality of X_{dc} with respect to E_{eff} with different substrate doping levels (from 10^{16} cm^{-3} to $3 \times 10^{18} \text{ cm}^{-3}$) is clearly shown in the Figure 1.

Usually, both the surface potential and depletion charge increment after strong inversion can be omitted in the conventional analytical models. However, the thickness of quantized inversion layer is larger than that of the semiclassical one, and as a result, the surface potential increases more than the semiclassical counterpart^[7]. Consequently, the depletion charge increases at the same time. The increment in the depletion charge after strong inversion is modelled below.

Since the total depletion charge is directly related to the surface potential induced by the depletion charge $\phi_{\text{s_dep}}$ as below:

$$Q_{\text{dep}} = \sqrt{2\epsilon_0\epsilon_{\text{Si}}\phi_{\text{s_dep}}/(q_0N_{\text{sub}})} \quad (9)$$

where N_{sub} is the substrate doping concentration, q_0 is the electron charge, so that we can model the overall $\phi_{\text{s_dep}}$ as:

$$\phi_{\text{s_dep}} = \phi_{\text{s_weak}} + \phi_{\text{s_inc}} \quad (10)$$

where $\phi_{\text{s_weak}}$ is the surface potential before strong inversion in conventional model:

$$\phi_{\text{s_weak}} = \left[\left(\sqrt{b^2 - 4V_{\text{g_weak}} - b} - b \right) / 2 \right]^2 \quad (11)$$

with $b = \sqrt{2\epsilon_{\text{Si}}N_{\text{sub}}q_0/\epsilon_0T_{\text{ox}}/\epsilon_{\text{SiO}_2}}$. In Eq. 11, $V_{\text{g_weak}}$ is given as:

$$V_{\text{g_weak}} = f - \sqrt{f^2 - V_{\text{gate}}V_{\text{th}}} \quad (12)$$

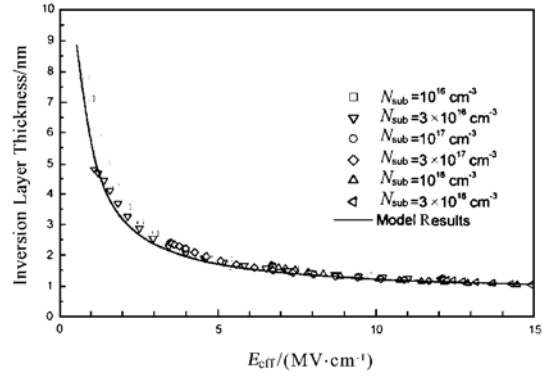


FIG. 1 Inversion Layer Thickness with Respect to Effective Electric Field. Symbols represent numerical results by self-consistent solution of Schrodinger and Poisson equations. Line represents model results. E_{eff} is given by Eq. 7 in the content.

with $f = 0.5(V_{\text{gate}} + (1 + \delta)V_{\text{th}})$. δ is a small quantity.

Based on the analysis of the underlying physics and the numerical results, the additional increment in surface potential due to the depletion charge can be modelled as:

$$\phi_{s_inc} = a_1(C_{\text{gate}}V_{\text{gtx}}/Q_{\text{dep0}})/(1 + a_2C_{\text{gate}}V_{\text{gtx}}/Q_{\text{dep0}}) \quad (13)$$

where Q_{dep0} is the depletion charge at the strong inversion point. C_{gate} is obtained from Eq. 2 by omitting the influence of ϕ_{s_inc} . $a_1 = 1.55$ and $a_2 = 10$ are determined by fitting the model results with the numerical ones.

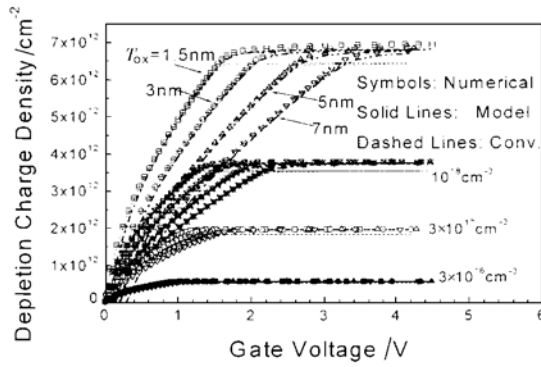


FIG. 2 Depletion Charge Density with Respect to Gate Voltage. Symbols stand for the numerical results while solid lines for model results. Different symbols are for those with different gate oxide thickness. Symbols with different interiors are at different substrate doping levels, as indicated in the Figure. Conventional model results without consideration of the increment of depletion charge after strong inversion are shown for comparison.

induced by the omission of the influence of ϕ_{s_inc} are non-negligible.

The threshold voltage in the above calculations are comprised of a conventional threshold voltage term and an additional quantum mechanical shift term^[5] given by:

$$V_{\text{th}} = V_{\text{th_conv}} + V_{\text{th_shift}} \quad (14)$$

with:

$$V_{\text{th_conv}} = V_{\text{FB}} + \phi_{s0} + \gamma \sqrt{\phi_{s0}} \quad (15)$$

and:

$$V_{\text{th_shift}} = \Delta\phi_s^m \left[1 + \frac{1}{2C_{\text{OX}}} \sqrt{\frac{\epsilon_0 \epsilon_{\text{Si}} q_0 N_{\text{sub}}}{\phi_{\text{th}} \ln(N_{\text{sub}}/n_i)}} \right] \quad (16)$$

where n_i is the intrinsic carrier concentration. The surface potential increment term $\Delta\phi_s^m$ is given by:

$$\Delta\phi_s^m = \frac{(\Delta E_{N_c} + E_{10})}{q} \quad (17)$$

in which ΔE_{N_c} is the density-of-states term and E_{10} is the band gap widening term^[5] and

The modelled depletion charge Q_{dep} (Eq. 12) and the numerical results by solving Schrodinger and Poisson equations are shown in Fig. 2. It is shown that within a wide range of the substrate doping levels (from $3 \times 10^{16} \text{ cm}^{-3}$ to $3 \times 10^{18} \text{ cm}^{-3}$) and gate oxide thickness (from 1.5 nm to 7 nm), the model results are coincident with the numerical ones very well. Also shown are the conventional model omitting the influence of ϕ_{s_inc} (It is useless to take the threshold voltage shift due to QMEs into consideration during the calculation of conventional model results). It is clearly indicated that at high substrate doping levels, the errors

given respectively by:

$$\Delta E_{N_c} = -k_B T \ln(N_{\text{eqm}}/N_{\text{class}}) \quad (18)$$

$$E_{10} = \left[\frac{\hbar^2}{2m_1} \right]^{1/3} \left[\frac{9}{8} \pi q_0 F_s \right]^{2/3} \quad (19)$$

where N_{eqm} and N_{class} are the quantum mechanical and semiclassical Surface Layer Effective Density-of-States (SLEDOS) respectively^[5], F_s is the surface electric field at threshold voltage.

Though the concept of Space Charge Capacitance (SCC) is applicable in all bias regions in MOS structures, it is of no sense to model the inversion layer thickness or the overall SCC in the depletion and weak inversion region. Alternatively, we adopt the well-known formula for carrier sheet density in a sub-threshold region^[11]:

$$Q_{\text{inv-sub}} = \sqrt{2\epsilon_0\epsilon_{\text{Si}}N_{\text{sub}}/(2\phi_{s0})} \phi_s \exp((V_{\text{gate}} - V_{\text{th}} - V_{\text{off}})/(\eta\phi_s)) \quad (20)$$

where V_{off} represents the small difference between the threshold voltages in the strong inversion and the subthreshold regions.

In order to get a unified formula for the charge sheet density from subthreshold to the strong inversion region, we introduce the effective gate voltage as:

$$V_{\text{gsteff}} = \frac{2\eta\phi_{\text{in}} \left[1 + \exp\left(\frac{V_{\text{gate}} - \phi_s - Q_{\text{dep}}/C_{\text{ox}}}{2\eta\phi_s}\right) \right]}{1 + 2\eta C_{\text{ox}} \sqrt{\frac{2\phi_{s0}}{q_0\epsilon_0\epsilon_{\text{Si}}N_{\text{sub}}}} \exp\left(\frac{V_{\text{gate}} - \phi_s - Q_{\text{dep}}/C_{\text{ox}} - 2(V_{\text{gate}} - V_{\text{th}} - V_{\text{off}})}{2\eta\phi_s}\right)} \quad (21)$$

Then, the inversion charge density can be expressed as:

$$Q_{\text{inv}} = C_{\text{ox}} V_{\text{gsteff}} \quad (22)$$

3 Model Results and Discussions

The calculated surface potential of the model is shown in Fig. 3 together with the numerical results. Different symbols represent different substrate doping levels and different gate oxide thickness in numerical results. Solid symbols are the substrate doping concentration of $3 \times 10^{16} \text{ cm}^{-3}$, while empty symbols are that of $3 \times 10^{17} \text{ cm}^{-3}$, and symbols with cross inside are that of $3 \times 10^{18} \text{ cm}^{-3}$. Squares represent the results with gate oxide thickness of 3nm, circles 5nm and triangles 7nm. Lines represent the model results indicated in the legend. For comparison, results from the conventional model are also shown in the Figure by lines with asterisks on them, not considering the inversion layer thickness and the depletion charge increase after strong inversion. The threshold voltage shift effect due to QMEs is included in the conventional results.

It indicates that in a wide range of substrate doping levels and the gate oxide thickness, the model results are satisfactorily coincident with the numerical results. It is also shown that even if the threshold voltage shift is included, the conventional model could have significant errors in the strong inversion region. The large increment in surface po-

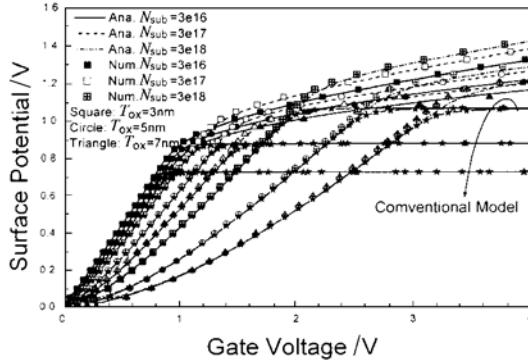


FIG. 3 Surface Potential of Inversion Layer in MOS Structure with Respect to Gate Voltage. Numerical results with different gate oxide thickness and substrate doping levels. Lines are model results self-consistent solution with the Schrodinger and Poisson equations.

tential is due to the finite inversion layer thickness (even larger in the quantized inversion layer) and the increment in depletion charge density. As far as we know, no such an analytical model of surface potential has been developed by accurately considering the two effects in the quantized inversion layer.

Inversion carrier sheet densities in linear and logarithmic scale are shown in Fig. 4(a) and (b), respectively. The meaning of symbols and lines are same as that in Fig. 3. The high accuracy as well as the smooth transition characteristics of

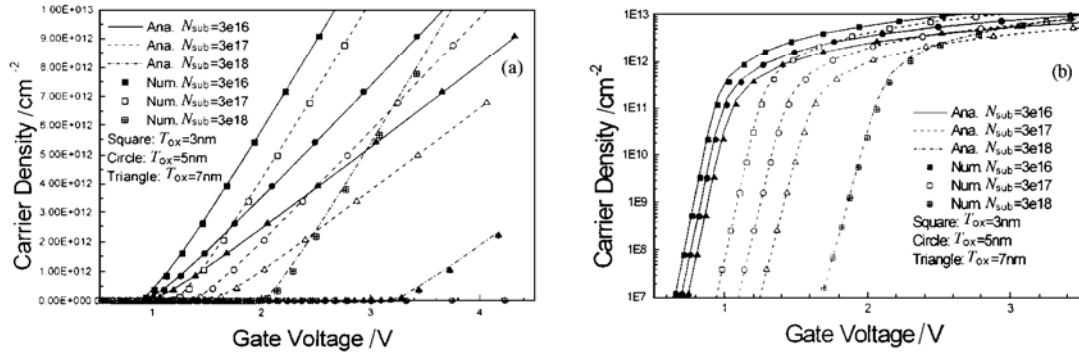


FIG. 4 Inversion Layer Carrier Density in MOS Structure with Respect to Gate Voltage. Lines are model results. (a) linear scale, (b) logarithmic scale.

4 Conclusions

The concept of Space Charge Capacitance (SCC) is used to build up a new analytical charge model of quantized inversion layer in MOS structure. Analytical formula for inversion layer thickness and depletion charge density are derived from the physical analysis and numerical data fitting. Explicit expressions of surface potential and inversion layer carrier density are given which have smooth transition characteristics from depletion to weak and strong inversion regions. Surface potential increment due to the finite inversion layer thickness and the depletion charge increment has been analyzed. Model results are compared with the numerical data by self-consistent solution to the Schrodinger and Poisson equation and the high accuracy of the model is verified.

References

- [1] F. Stern, Phys. Rev. B, 1972, **5**(12): 4891.
- [2] T. Ando, A. B. Fowler and F. Stern, Rev. Mod. Phys., 1982, **54**: 437—672.
- [3] Wei Deng, Lilin Tian and Yutao Ma, "Rigorous Numerical Study of Quantum Mechanical Effects in Ultra-Small MOS Devices", Submitted to Chinese Journal of Semiconductors.
- [4] C. Chindalore, S. A. Hareland, S. Jallepalli, A. F. Tasch, Jr., C. M. Maziar, V. K. F. Chia and S. Smith, IEEE EDL, 1997, **18**(5): 206—208.
- [5] Yutao Ma, Zhijian Li and Litian Liu, Chinese Journal of Semiconductors, 1999, **20**(3): 219.
- [6] Weidong Liu, Xiaodong Jin, Yachin King and Chenming Hu, IEEE Trans. on Electron Devices, 1999, **46**(5): 1070.
- [7] Tomasz Janik and Bogdan Majkusiak, IEEE Trans. on Electron Devices, 1998, **45**(6): 1263.
- [8] Rafael Rios, Narain D. Arora *et al.*, IEDM 95, 1995, 937.
- [9] M. J. van Dort, P. H. Woerlee and A. J. Walker, Solid-State Electron., 1994, **37**(3): 435.
- [10] Cheng Yuhua, Chen Kai, Imai Kiyotaka and Hu Chenming, SISPAD'97, 1997, 109—112.
- [11] Yuhua Cheng, Jeng Min-Chie, Liu Zhihong, Huang Jianhui, Chan Mansun, Chen Kai, Ko Ping Keung and Hu Chenming, IEEE Trans. ED., 1997, **44**(2): 277—287.